Tetrahedron Vol. 36, pp. 1317 to 1326
© Pergamon Press Ltd., 1980. Printed in Great Britain

0040-4020/80/0515-1317/$02.00/0

MO- AND VB-BENZENE CHARACTERS

ANALYSIS OF THE "CLAR'S AROMATIC SEXTET" IN POLYCYCLIC AROMATIC HYDROCARBONS

MISAKO AIDA and HARUO HOSOYA*
Department of Chemistry, Ochanomizu University, Bunkyo-Ku, Tokyo 112, Japan

(*Received in Japan* 19 *October* 1979)

Abstract—In order to analyse the mode of distribution of π-electrons in a given hexagon in a polycyclic aromatic hydrocarbon, normalised VB- and MO- (HMO and PPP) benzene characters are defined and calculated for a number of molecules. Their relation to the topological structure of the molecule was studied in detail. By combining these quantities it was shown that the π-electrons in the three different classes (primary, secondary and tertiary) of hexagons have different distribution over the benzene ring. It was found that the value of the benzene character is determined by the local topological structure up to the third next hexagons. These findings qualitatively support and quantitatively figure out the concept of the Clar's aromatic sextet, which can be interpreted as the "higher order π-electronic correlation" that the π-electronic system of polycyclic aromatic hydrocarbons can be described by the cooperative interaction of the units of closely correlated six π-electrons.

The relative stabilities of isomeric polycyclic aromatic hydrocarbons are attributed to the difference in the total π-electronic energy, E_π, which is a function of the topological structure of the component hexagons. Several empirical formulas hitherto proposed[1-3] suggest that E_π can be expressed as the sum of the contributions of some unknown "benzene character" over the component hexagons. However, little is known about the details of this functional form, albeit a number of sophisticated calculations can afford fairly accurate prediction on the electronic structures of individual polycyclic aromatic hydrocarbons.[4-8]

On the other hand, it has been known empirically that the "angular annellation", "phene structure", or "kink" as in phenanthrene

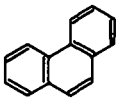

yields extra stabilisation energy relative to the linear "acene structure",[9]

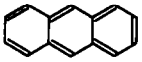

According to the Clar's postulate of the "aromatic sextet",[10] the above argument is translated into the comparison of the maximum number of the resonant sextets as in

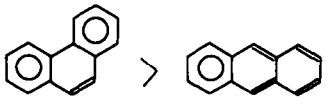

In this paper let us call these structures with the largest number of aromatic sextets as the "Clar patterns".

Polansky and Derflinger gave the MO interpretation of the aromatic sextet by defining a measure of the benzene character in terms of the Hückel molecular orbitals (HMO).[11,12] It is still an open question if these relations may or may not be changed as the improvement of the molecular orbitals.

Herndon and Ellzey,[15] Randić,[16] and Aihara[17] independently showed that the relative weight of each benzene ring in the enumeration of the Kekulé structures represents the Clar pattern and the relative aromatic character of the component rings fairly well. One of the present authors showed that by defining the sextet polynomial these resonance-theoretical or VB-theoretical quantities are interrelated to each other and also related to the number of the sextets in the Clar pattern.[18]

However, most of the discussions in these studies have been limited to the comparison or correlation of these quantities among certain series of compounds. The analysis of the relation between the topological structure and these quantities is also not yet fully given. The purposes of the present paper are to analyse the relation between these MO- and VB-benzene characters with particular reference to their topology dependency and also to see the effect of the degree of approximation in the MO calculation on the benzene character.

Definitions of benzene characters

MO-benzene characters.[11] Suppose a local structure L in a π-electronic conjugated molecule M, and calculate the MO's of molecule L and M. For example, L may be a particular bond (ethylene), three consecutive bonds (butadiene), or a hexagon (benzene) in naphthalene (M). By definition the Coulson bond orders for bond jk in molecules L and M are respectively obtained as:

$$p^L_{jk} = 2\sum_n^{occ} C^L_{nj}C^L_{nk} \tag{1}$$

$$p_{jk} = 2\sum_n^{occ} C_{nj}C_{nk}. \tag{2}$$

Polansky and Derflinger have shown that the projection of the occupied MO's in the local structure L of M onto the occupied MO's of molecule L is reduced to the quantity

$$r_L = \frac{1}{2n_L}\sum_j^{in\,L}\sum_k^{in\,L} p^L_{jk}p_{jk} \tag{3}$$

where n_L is the number of the C atoms in L. By using the charge density

$$q_j = 2\sum_n^{occ} C_{nj}^2 \tag{4}$$

r_L can be expressed as:

$$r_L = \frac{1}{2n_L}\sum_j^{n_L} q_j^L q_j + \frac{1}{n_L}\sum_{j<k}^{n_L} p_{jk}^L p_{jk} \tag{5}$$

where the double summation in the second term runs over all the atom pairs in L, irrespective of the adjacency relation between j and k. For an alternant hydrocarbon the pairing theorem ensures that:

$$r_L = \frac{1}{2} + \frac{1}{n_L}\sum_{j<k}^{n_L} p_{jk}^L p_{jk}. \tag{6}$$

The Hückel MO's (HMO) of benzene give the following values

$$p_{ortho}^L = 2/3, \quad p_{meta}^L = 0, \quad p_{para}^L = -1/3,$$

and for a particular benzene ring L in molecule M we have

$$r_L = \frac{1}{2} + \frac{1}{18}\left(2\sum^{ortho} p_{ortho} - \sum^{para} p_{para}\right). \tag{7}$$

Polansky and Derflinger[11] have calculated the values of r_L for a number of polycyclic aromatic hydrocarbons and have shown that r_L varies in the range 0.8–1.0, with the maximum value of 1.0 for benzene.[a] However, it turns out that r_L is as high as 5/6 for a set of three isolated double bonds. Then let r_L be transformed into $\bar{r}_L$ as

$$\bar{r}_L = 6r_L - 5 \tag{8}$$

$$= \frac{1}{3}\left(2\sum^{ortho} p_{ortho} - \sum^{para} p_{para}\right) - 2$$

so as to vary from 0 for three isolated double bonds to 1.0 for benzene, and call it as (normalised) MO-benzene character.

In this paper two different sets of MO-benzene characters $\bar{r}_L^H$ and $\bar{r}_L^P$ for a number of polycyclic aromatic hydrocarbons were calculated by using the HMO and variable-β version of the PPP MO's.[19]

VB-benzene character. Let K(G) be the number of the Kekulé structures of graph G, and $G\ominus R_L$ be the subgraph of G obtained by deleting ring R_L together with all the bonds adjacent to R_L.[20] Then the quantity

$$b_L = 2K(G\ominus R_L) \tag{9}$$

is nothing else but the number of the Kekulé structures in which a set of circularly resonating three double bonds can be drawn in a particular hexagon R_L. Note the schematic relation below

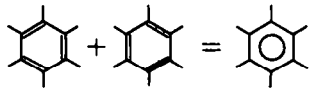

The quantity b_L has the values 2 and 0, respectively, for benzene and the central hexagon in perylene where no sextet can be drawn. Thus the following quantity is defined as the normalised VB-benzene character

$$\bar{b}_L = \frac{2K(G\ominus R_L)}{K(G)}, \tag{10}$$

[a] In their papers the values $\rho_L = 2(r_L - (1/2))$ are given, which is supposed to take the value between −1 and 1 for the range between 0 and 1 of r_L. The relation between $\bar{r}_L$ and ρ_L is $\bar{r}_L = 3\rho_L - 2$.

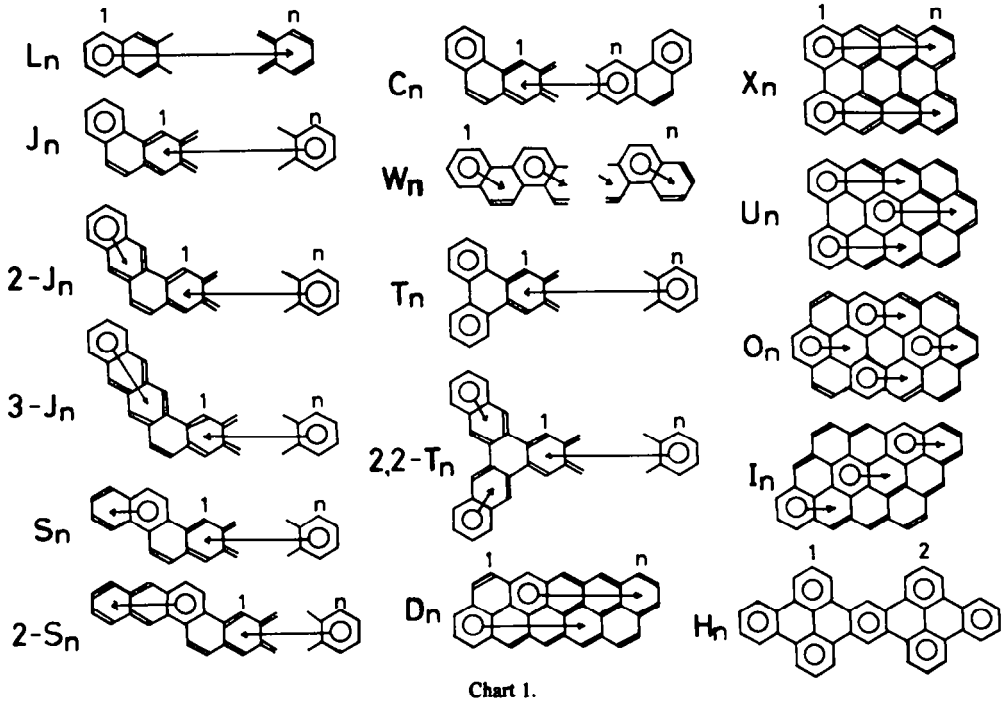

Chart 1.

which takes the values of 1 and 0, respectively, for benzene and a set of three isolated double bonds. The number of the Kekulé structures for a conjugated hydrocarbon can be obtained by the successive application of the recurrence formulas.[13-18]

RESULTS

General remarks. In this paper the three different benzene characters, $\bar{r}_L^H$, $\bar{r}_L^P$ and $\bar{b}_L$, have been calculated for all the members of the polycyclic aromatic hydrocarbons with up to six hexagons and several series of hydrocarbons as shown in Charts 1–3, where one of the typical Clar patterns and tentative symbols representing the shape and size of the molecule are given.

For pentacene (L_5) three benzene characters are given in Fig. 1. It has been known that for polyacene and other hydrocarbon molecules with a long polyacene moiety the set of the Kekulé structures alone is not good enough for explaining the π-electronic properties of the ground state of these molecules. Namely, a single Clar's aromatic sextet is delocalised equally with the weight of $\bar{b}_L = 2/(n+1)$ all over the long chain of benzene rings

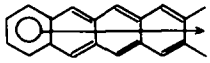

but excludes the coexistence of other sextets to gain additional stability no matter what the size of the molecule increases. Then the value $\bar{b}_L$ converges to zero for an infinitely long polyacene. This means that the stabilisation energy of these types of molecules is underestimated as long as only the Kekulé structures are taken into account.

Fig. 1. Three benzene characters, $\bar{b}_L$(VB), $\bar{r}_L^H$(HMO) and $\bar{r}_L^P$(PPP), of pentacene (L_5).

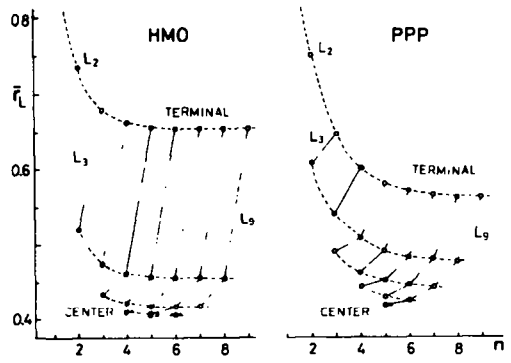

Fig. 2. Dependency of the $\bar{r}_L^H$ and $\bar{r}_L^P$ values for polyacenes on the site of the hexagon (—) and on the size of the molecule (---). The benzene characters are the largest for the terminal hexagons and monotonously decrease toward the center of the molecule. The value of the benzene character for the terminal hexagon of polyacene (L_n) with n hexagons is plotted above the abscissa n. See also Table 1 and Fig. 1.

On the other hand, the distribution of the values of $\bar{r}_L^H$ and $\bar{r}_L^P$ are very similar as is also shown in Fig. 2, where these values for the polyacene series (L_2–L_9) are plotted. The benzene characters $\bar{r}_L^H$ and $\bar{r}_L^P$ are the largest at the terminal ring p_n, sharply drop at the next ring and slowly decrease toward the center s. These limiting values gradually decrease with the size of the molecule but, contrary to the VB-benzene character, converge to certain values. The rate of the convergence is faster for the $\bar{r}_L^H$ value than for the $\bar{r}_L^P$. (Table 1).

Now to turn to other examples, Fig. 3 gives the benzene characters of anthanthrene (D_3). It is remarkable in this case that the distribution of the $\bar{b}_L$ values agrees well with that of $\bar{r}_L^P$, but deviates slightly from that of $\bar{r}_L^H$. The results of the zig-zag series (W_n) are given in Fig. 4, where again $\bar{b}_L$ gives similar distribution with that of $\bar{r}_L^P$ but $\bar{r}_L^H$ shows smooth distribution. From the examination of a number of plots[21] it is concluded that except for polyacene-like molecules the $\bar{b}_L$ values, which can be obtained by a hand calculation, can be used as a rough estimation of the $\bar{r}_L^P$ values.

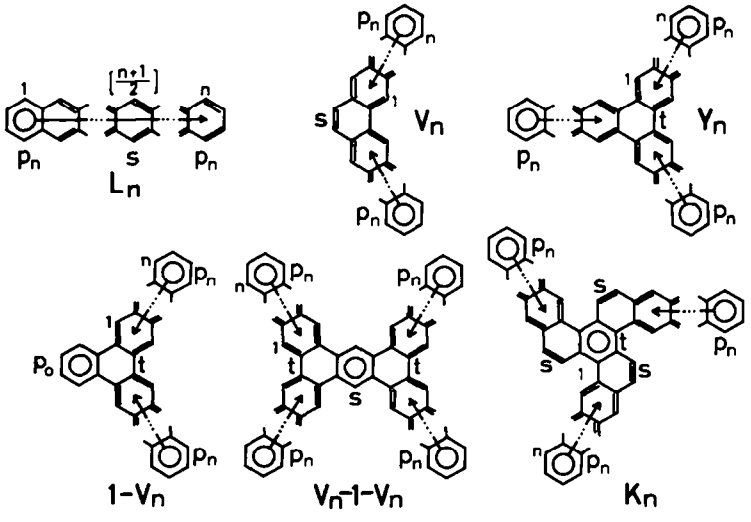

Chart 2.

Table 1. Benzene characters of typical series of catafusenes having extremum values for primary catahexes

Series[a]	L_n				$1-V_n$					
n	p_n		s		p_o		t		p_n	
	$\bar{r}_L^H$	$\bar{r}_L^P$	$\bar{r}_L^H$	$\bar{r}_L^P$	$\bar{r}_L^H$	$\bar{r}_L^P$	$\bar{r}_L^H$	$\bar{r}_L^P$	$\bar{r}_L^H$	$\bar{r}_L^P$
1	1.000	1.000	1.000	1.000	0.821	0.869	0.141	0.089	0.821	0.869
2	0.735	0.750	0.735	0.750	0.829	0.885	0.025	-0.118	0.712	0.726
3	0.678	0.647	0.518	0.600	0.829	0.887	-0.006	-0.192	0.676	0.643
4	0.663	0.602	0.475	0.541	0.828	0.888	-0.015	-0.221	0.663	0.601
5	0.657	0.581	0.434	0.492	0.827	0.888	-0.018	-0.234	0.658	0.581
6	0.656	0.571	0.422	0.466	0.827	0.888	-0.018	-0.240	0.656	0.571
7	0.655	0.566	0.411	0.443	0.827	0.888	-0.018	-0.243	0.655	0.566
8	0.655	0.564	0.408	0.432	0.827	0.888	-0.018	-0.244	0.655	0.564
9	0.655	0.563	0.405	0.421	0.826	0.888	-0.016	-0.244	0.655	0.563
10	0.655	0.562	0.404	0.415						
20	0.655	0.562	0.401	0.400						
∞[c]	0.655[b]	0.562	0.401	0.398	0.826	0.888	-0.016	-0.244	0.655	0.562
$\bar{b}_L$	$\frac{2}{n+1} \to 0$		$\frac{2}{n+1} \to 0$		$\frac{2(n+1)^2}{2(n+1)^2+1} \to 1$		$\frac{2}{2(n+1)^2+1} \to 0$		$\frac{4(n+1)}{2(n+1)^2+1} \to \frac{2}{n+1} \to 0$	

a) See Chart 1. b) Underlines and overlines, respectively, indicate the lowest and highest limits for the primary catahexes.

c) Estimated values.

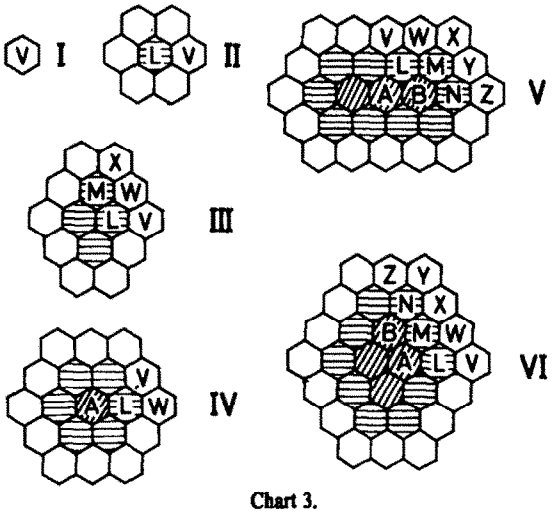

Chart 3.

In general the PPP method, thanks to its explicit inclusion of the electronic repulsion, would give fairly reliable information on the distribution of electrons. However, the complicated SCF procedure prevents us from deriving analytic expressions for several important

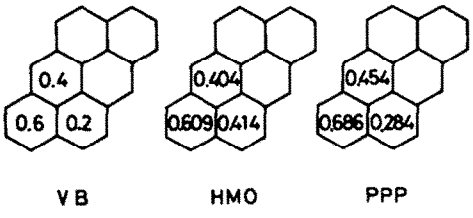

Fig. 3. Three benzene characters of anthanthrene (D_3).

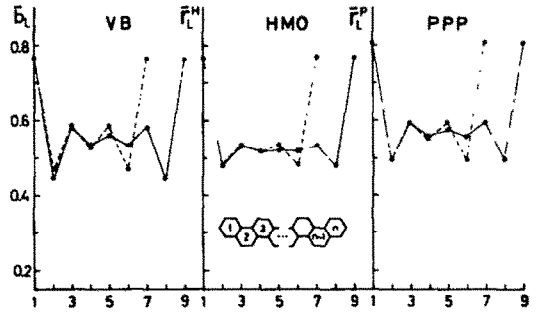

Fig. 4. Three benzene characters of "zig-zag" polycyclic aromatic hydrocarbons (W_7 and W_9).

quantities, and gives us only vague information regarding the infinitely large π-electronic systems in the case where the quantity concerned changes slowly with the size of the molecule. The advantage of the HMO calculation over more accurate methods at the sacrifice of the precision lies in its mathematical neatness and smaller amount of computation to be needed. Thus from now on we will use $\bar{r}_L^H$ and $\bar{r}_L^P$ complementarily for the detailed analysis of the benzene characters in relation to the topological structure of the molecule. The complementary character of these two quantities will be clear from Fig. 5, where the $\bar{r}_L^P$ values are plotted against the $\bar{r}_L^H$ values for all the catacondensed aromatic hydrocarbons studied.

Classification of benzene rings. Polycyclic aromatic hydrocarbons are largely classified into catacondensed and pericondensed aromatic hydrocarbons. In this paper we will call them, respectively, as catafusenes and perifusenes after Balaban and Harary.[22] If we are concerned with the benzenoid aromatics which are composed only

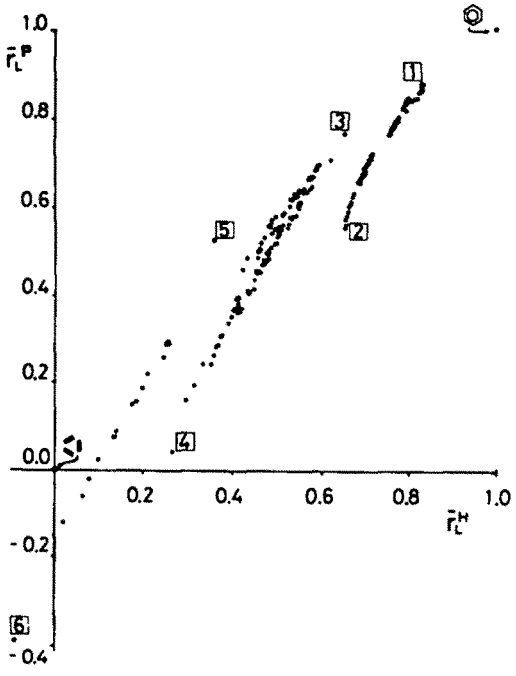

Fig. 5. The plot of $(\bar{r}_L^H, \bar{r}_L^P)$ for catafusenes (catacondensed aromatic hydrocarbons). Except for benzene (1,1) and a set of three isolated double bonds (0,0), the benzene rings are grouped into three classes of plots, i.e. primary between 1 and 2, secondary between 3 and 4 and tertiary between 5 and 6. 1: p_0 of $1 - V_\infty$, 2: p_n of L_∞, 3: s of $V_\infty - 1 - V_\infty$, 4: s of V_∞, 5: t of K_∞, and 6: t of Y_∞. See Chart 2 and Tables 1, 3 and 4 for notations.

of hexagons, they can be represented simply by their skeletal graph whose points are the centers of the component hexagons and whose lines represent their connectivity. With this skeletal graph expression catafusenes and perifusenes are, respectively, tree and non-tree graphs.

Let the component hexagons of catafusenes be called as catahexes and those of perifusenes as perihexes. Both of them are further classified as in Table 2 depending on the number (degree) of the adjacent hexagons. If the directions of branching are also taken into account we have four different types of catahexes as

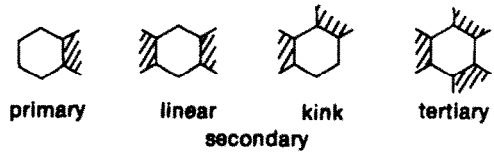

For perifusenes there are eight types of perihexes for which hieroglyphic symbols are given in Table 2.

Although it has been known empirically that the electronic properties, such as bond order and carcinogenic activity,[23] of the component benzene rings in polycyclic systems seem to depend on the environmental arrangement of other hexagons, systematic analysis has not yet been performed.[12] It was found in this study that by combining the benzene characters of $\bar{r}_L^H$ and $\bar{r}_L^P$ one can clearly distinguish each type of hexagons, especially for catahexes. The factors governing the electronic properties of the component hexagons in polycyclic systems were also clarified.

As evident from Fig. 5 the plots of $\bar{r}_L^P$ against $\bar{r}_L^H$ except for the points (1,1) (benzene) and (0,0) (three independent double bonds) are sharply grouped into three sets of points lying on straight lines parallel to each other. The first group of points lying in between points 1 and 2 are nothing else but the primary catahexes. The groups in between 3 and 4 and 3 and 6 are, respectively, secondary and tertiary catahexes. Note that the value $\bar{r}_L^P$ alone cannot differentiate them effectively, while the $\bar{r}_L^H$ value can work fairly well but not perfectly.

(i) *Primary catahex.* Careful inspection of the plots in Fig. 5 reveals that the primary catahex plots are subdivided into five segments as of

This feature can also be seen in Fig. 6, where the histogram of the $\bar{r}_L^H$ values for the catahexes of the 77 catafusenes with up to six hexagons are given. Several peaks in the histogram of primary catahexes are found to correspond to finer subclasses. This means that the value of the benzene character $\bar{r}_L^H$ of a primary catahex can be predicted within an error of 0.03 if one knows the local

Table 2. Classification of catahexes and perihexes

	Degree					
	1	2	3	4	5	6
Catahex						
Perihex		 V	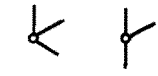 U 3 Y 2+1	 W 4 T 3+1 X 2+2	 Q	 O

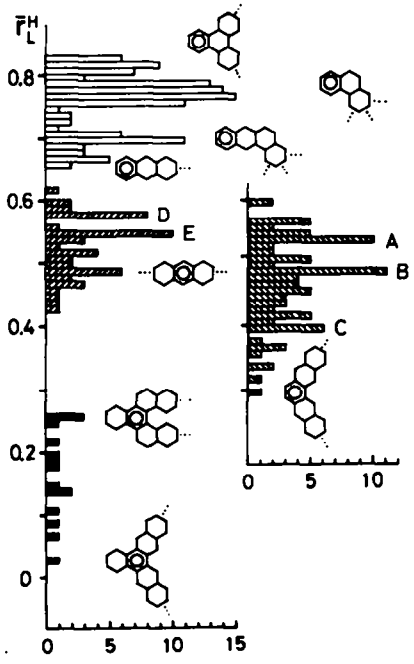

Fig. 6. Histogram of the $\bar{r}_L^H$ values for the catahexes of the 77 polycyclic aromatic hydrocarbons. □: primary catahex, ▨: linear secondary catahex, ▧: kink secondary catahex, ■: tertiary catahex. See text for A–E.

structure up to the third next hexagons around the hexagon concerned.

The above discussion has been obtained from the limiting number of relatively small polycyclic aromatic hydrocarbons. Question arises to what extent does this classification hold if one goes on to infinitely large systems. For this purpose the combination of $\bar{r}_L^H$ and $\bar{b}_L$ is found to be effective since the former gives analytical expression for the asymptotic behavior of the system

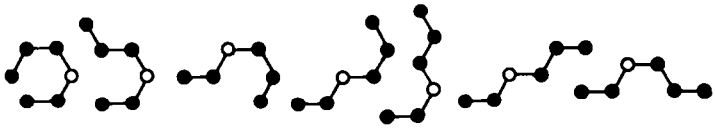

concerned and the latter presents its pictorial interpretation by the aid of the Clar patterns.

The analytical formula of ρ_L's have already been obtained by Sofar *et al.* for polyacenes (L_n) by using HMO wavefunctions.[12] As seen in Table 1 the $\bar{r}_L^H$ value for the terminal (primary) catahexes p_n almost converges at heptacene (L_7) to the value of 0.655 and the value for the central hexagons s of L_9 and L_{10} is very close to the limiting value of 0.401. On the other hand, the value of $\bar{r}_L^P$ shows slower convergence.

As has been pointed out earlier, for polyacene series the Clar pattern is not a good description for the ground state; every member of the hexagons of L_n having a uniform value of $\bar{b}_L = 2/(n+1)$. Anyway the limiting value 0.655 for the terminal hexagon p_n of L_n is the smallest value of $\bar{r}_L^H$ for the primary catahex. The corresponding $\bar{r}_L^P$ value is 0.562. This is plotted as point 2 in Fig. 5.

A symmetrically V shaped catafusene in which two L_n moieties are angularly joined to a hexagon may be called as V_n. Let us then call such a catafusene as $1-V_n$ that is composed of a hexagon and V_n as in Chart 2.

The protrudent hexagon p_0 of this molecule has a peculiar feature of its large benzene character. According to Clar, the ground state of $1-V_n$ can be expressed as the diagram in Chart 2 having three resonant sextets, two of which move across the long linear branches of hexagons leaving a large benzene character on the hexagon p_0. In other words, in each of the $2(n+1)^2$ Kekulé structures out of $2(n+1)^2+1$ an aromatic sextet can be drawn in the protrudent hexagon p_0.

The calculated values of $\bar{r}_L^H$ and $\bar{r}_L^P$ for p_0 are given in Table 1, from which the largest $\bar{r}_L^H$ value 0.829 for the primary catahex is found in $1-V_2$. All of the largest members of this series have similar values of p_0. In Fig. 5 the p_0 value for $1-V_\infty$ is plotted as point 1. On the other hand, the central hexagon t is expected to have very low $\bar{r}_L^H$ value, which, however, is not the smallest among the tertiary catahexes.

(ii) *Secondary catahex.* A number of subclasses mingle each other in the plot of the secondary catahexes in Fig. 5. One cannot tell the local structure around the secondary catahex concerned just by knowing the value of $\bar{r}_L^H$ above 0.4, but the $\bar{r}_L^H$ value between 0.3 and 0.4 is assigned to the "kink" hexagon at which two straight polyacene moieties (including the terminal hexagon) meet. However, if one plots the $\bar{r}_L^H$ values of "linear" and "kink" secondary catahexes separately as in Fig. 6, interesting features come out.

The main body of the peak A of the histogram of the kink group at 0.53–0.54 is the following class of isomers,

where an open circle represents the kink hexagon concerned. Note that these eight entries out of ten are the members of all the possible combinations obtained by joining two phenanthrene molecules so that the junction takes the kink form. The other two entries are as follows:

Quite similar classes of isomers are found in the peaks B($\bar{r}_L^H$ = 0.48–0.49)

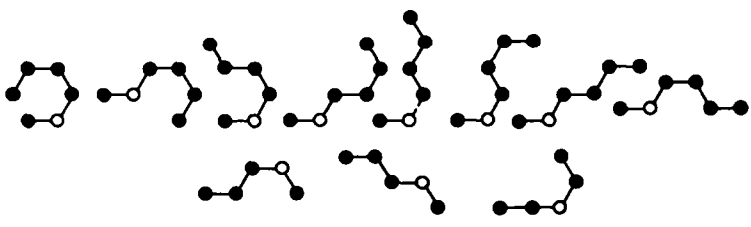

and C($\bar{r}_L^H$ = 0.39–0.40)

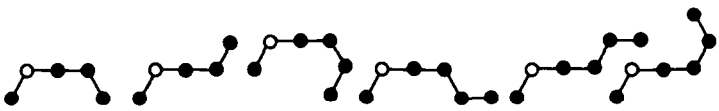

Most of the linear secondary catahexes in peaks D($\bar{r}_L^H$ = 0.57–0.58) and E($\bar{r}_L^H$ = 0.54–0.55) have common local structures, respectively, as

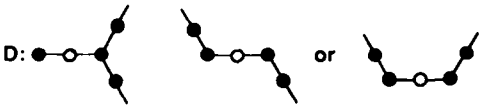

and

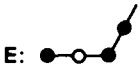

Linear secondary catahexes with the local structure as

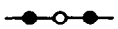

have the values of $\bar{r}_L^H$ = 0.42–0.52.

As deduced from the asymptotic behavior of the series L_n and $1-V_n$ the central catahex s in V_n is expected to have the smallest benzene character for the secondary catahexes. This is actually the case. The values are $\bar{r}_L^H$ = 0.266 and $\bar{r}_L^P$ = 0.043 (Table 3 and point 4 in Fig. 5).

By joining two V_n's linearly to a hexagon one gets a series of molecules V_n-1-V_n, whose Clar pattern has five resonant sextets as in Chart 2. The benzene character of all the hexagons in the four branches is diluted, whereas the central hexagon s is expected to have large $\bar{r}_L^H$ and $\bar{r}_L^P$ values. Actually the values, $\bar{r}_L^H$ = 0.633 for V_2-1-V_2 and $\bar{r}_L^P$ = 0.776 for $V_\infty-1-V_\infty$ are found to be the maxima for the secondary catahexes (Table 3 and point 3 in Fig. 5).

(iii) *Tertiary catahex.* Starphene Y_n is composed of three arrays of L_n moieties and the central hexagon t, whose benzene character is found to be the smallest of the tertiary catahexes. Therefore the ground state of starphene may be represented as in Chart 2 where three sextets of triphenylene move across the L_n moieties. It is to be noted that the limiting value of −0.380 for $\bar{r}_L^P$ is rather small compared to that of $\bar{r}_L^H$ of −0.087 (Table 4 and point 6 in Fig. 5). Generally the PPP method gives the values of higher contrast than the HMO method for the benzene character. This reminds us of the similar features of the bond order for the large acyclic π-electronic networks.[24]

The propeller-shaped polyhex K_n has the same components as Y_n, the only difference being in the direction of branching. However, this difference is crucial for determining the number of the kink hexagons. A sextet moves across each of the three L_n branches, leaving the fourth sextet fixed on the central hexagon t and thus placing there a large benzene character. The largest $\bar{r}_L^H$ and $\bar{r}_L^P$ values for the tertiary catahexes are found to be, respectively, 0.360 and 0.530 for the t hexagon of the infinitely large molecule K_n (Table 4 and point 5 in Fig. 5).

(iv) *Perihex.* In Fig. 7 are plotted the $\bar{r}_L^H$ values of perihexes from the nineteen perifusenes having four to six hexagons and a singlet ground state. They are separately plotted according to the classification of Table 2. The value of $\bar{r}_L^H$ smoothly changes with the number of the neighbouring hexagons, but their distinction is not so clear as in the case of catahexes. The $\bar{r}_L^H$ values of the first class V with two neighbours range from 0.6 to 0.72.

Table 3. Benzene characters of typical series of catafusenes having extremum values for secondary catahexes

Series[a]	V_n				V_n-1-V_n					
	s		p_n		s		t		p_n	
n	$\bar{r}_L^H$	$\bar{r}_L^P$	$\bar{r}_L^H$	$\bar{r}_L^P$	$\bar{r}_L^H$	$\bar{r}_L^P$	$\bar{r}_L^H$	$\bar{r}_L^P$	$\bar{r}_L^H$	$\bar{r}_L^P$
1	0.439	0.422	0.783	0.825	0.652	0.749	0.115	0.053	0.822	0.872
2	0.316	0.194	0.701	0.705	0.663	0.771	0.006	−0.136	0.712	0.726
3	0.281	0.108	0.673	0.634	0.660	0.775	−0.023	−0.205	0.676	0.643
4	0.271	0.073	0.662	0.597	0.658	0.775	−0.031	−0.233	0.663	0.601
5	0.267	0.057	0.658	0.579						
6	0.266	0.050	0.656	0.570						
7	0.266	0.047	0.656	0.566						
8	0.266	0.045	0.655	0.564						
∞[c]	0.266[b]	0.043	0.655	0.562	0.655	0.776	−0.035	−0.244	0.655	0.562
E_L	$\frac{2}{(n+1)^2+1} \to 0$		$\frac{2(n+1)}{(n+1)^2+1} \to \frac{2}{n+1} \to 0$		$\frac{(n+1)^2}{(n+1)^2+1} \to 1$		$\frac{1}{(n+1)^2+1} \to 0$		$\frac{2(n+1)^2+1}{(n+1)\{(n+1)^2+1\}} \to \frac{2}{n+1} \to 0$	

a) See Chart 1. b) Underlines and overlines, respectively, indicate the lowest and highest limits for the secondary catahexes. c) Estimated values.

Table 4. Benzene characters of typical series of catafusenes having extremum values for tertiary catahexes

Series[a]	Y_n				K_n					
n	t		p_n		t		s		p_n	
	$-\bar{r}_L^H$	$\bar{r}_L^P$	$\bar{r}_L^H$	$\bar{r}_L^P$	$\bar{r}_L^H$	$\bar{r}_L^P$	$\bar{r}_L^H$	$\bar{r}_L^P$	$\bar{r}_L^H$	$\bar{r}_L^P$
1	0.141	0.089	0.821	0.869	0.141	0.089			0.821	0.869
2	-0.030	-0.212	0.714	0.732	0.316	0.391	0.513	0.538	0.762	0.794
3	-0.072	-0.311	0.677	0.646	0.351	0.478	0.441	0.402	0.691	0.678
4	-0.084	-0.350	0.663	0.603	0.359	0.509	0.419	0.345	0.668	0.618
5	-0.086	-0.366	0.658	0.582	0.360	0.521	0.412	0.320	0.660	0.589
6	-0.087	-0.373	0.656	0.572	0.360	0.526	0.409	0.308	0.657	0.575
∞[c]	-0.087[b]	-0.380	0.655	0.562	0.360	0.530	0.407	0.298	0.655	0.562
$\bar{b}_L$	$\frac{2}{(n+1)^3+1} \to 0$		$\frac{2(n+1)^2}{(n+1)^3+1} \to \frac{2}{n+1} \to 0$		$\frac{2n^3}{(n+1)^3+n^3} \to 1$		$\frac{2(n+1)^2}{(n+1)^3+n^3} \to \frac{1}{n+1} \to 0$		$\frac{2\{(n+1)^2+n^2\}}{(n+1)^3+n^3} \to \frac{2}{n+1} \to 0$	

a) See Chart 1. b) Underlines and overlines, respectively, indicate the lowest and highest limits for the tertiary catahexes. c) Estimated values.

Those perihexes with relatively large $\bar{r}_L^H$ values (0.4–0.6) mostly belong to class U, in which three neighbours are joined to each other, while those with smaller $\bar{r}_L^H$ (0.26–0.44) to class Y, in which the three neighbours are grouped into two and one. The hexagons of class T with 3+1 neighbours have small $\bar{r}_L^H$ values around 0.1–0.2. As the number of the examples of other classes W (with four neighbours), X (with 2+2 neighbours) and those with more than five neighbours are limited, no general tendency could be obtained. However, as in the plot of Fig. 5 for catahexes the $\bar{r}_L^P$ values of perihexes are also found to be correlated well with the $\bar{r}_L^H$ values.

Bradburn *et al.* estimated the limiting value of the bond order in the graphite network to be 0.525.[25] However, it is difficult to obtain the value for the 1–4 atom pair. Therefore we have performed the HMO and PPP calculations for the large "2-dimensional" networks as shown in Chart 3. As seen in Table 5, the benzene character is fairly large for the outermost shell, sharply drops in the second shell, ripples and converges to a

Table 5. The MO-benzene characters $\bar{r}_L^H$ and $\bar{r}_L^P$ (in parentheses) for round-shaped perifusenes

Hexagon[a]		Molecule[a]				
		II	III	IV	V	VI
Third Shell	A			0.329 (0.436)	0.301 (0.378)	0.288 (0.265)
	B				0.300 (0.317)	0.312 (0.404)
	Mean[b]			0.329 (0.436)	0.300 (0.337)	0.300 (0.335)
Second Shell	L	0.260 (0.119)	0.314 (0.339)	0.285 (0.225)	0.286 (0.221)	0.314 (0.382)
	M		0.270 (0.152)		0.304 (0.346)	0.281 (0.208)
	N				0.279 (0.178)	0.289 (0.242)
	Mean	0.260 (0.119)	0.292 (0.245)	0.285 (0.225)	0.292 (0.262)	0.291 (0.257)
Outermost Shell	V	0.510 (0.554)	0.403 (0.291)	0.418 (0.534)	0.353 (0.444)	0.386 (0.237)
	W		0.410 (0.504)	0.425 (0.372)	0.364 (0.403)	0.368 (0.409)
	X		0.477 (0.510)		0.399 (0.268)	0.385 (0.490)
	Y				0.404 (0.494)	0.416 (0.350)
	Z				0.442 (0.460)	0.411 (0.528)
	Mean	0.510 (0.554)	0.435 (0.464)	0.421 (0.453)	0.391 (0.404)	0.392 (0.408)

a) See Chart 3 b) Weighted mean.

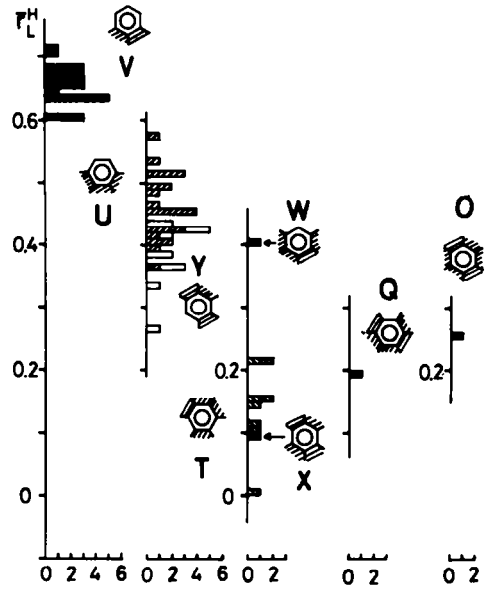

Fig. 7. Histogram of the $\bar{r}_L^H$ values for the perihexes of the nineteen perifusenes. Refer to Table 2 for the notations.

certain limit as we go into the center of the network. It seems from Table 5 that the limiting value is as large as $\bar{r}_L^H = 0.300$ and $\bar{r}_L^P = 0.33$ for the benzene character of the graphite network.

Structural factors determining the benzene character. As has been shown in a number of examples above the benzene character of a given hexagon in a given polycyclic system is determined by the local structure around it. More dramatic examples are shown in Fig. 8, where the $\bar{r}_L^P$ values of the component hexagons of such six

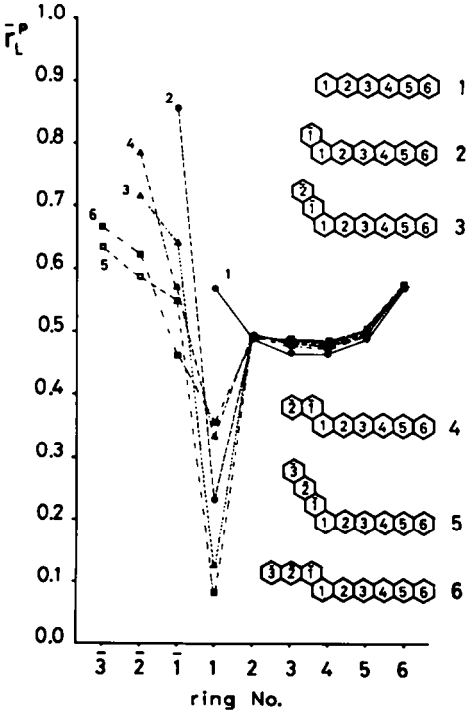

Fig. 8. The $\bar{r}_L^P$ values for several catafusenes with pentacene moiety. 1: L_6, 2: J_5, 3: 2-J_5, 4: S_5, 5: 3-J_5, 6: 2-S_5. See Chart 1 for the notations.

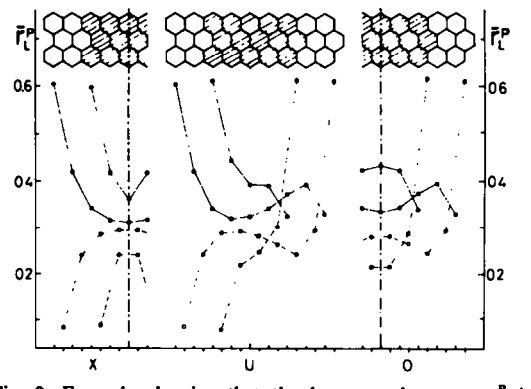

Fig. 9. Example showing that the benzene character $\bar{r}_L^P$ is determined by the local topological structure. Molecules X_n and O_n are symmetric and U_n is a hybrid of X_n and O_n. O: molecules with n = 9, ●: molecules with n = 5 (shaded), —: peripheral hexagons, —: inner hexagons.

catafusenes are plotted and compared with each other that have a pentacene moiety in common. If one deletes pentacene from this group, for the rest of the compounds the structure up to the seventh hexagon (ring number $\bar{1}$) counting from one (6) of the terminals is in common and the values of the benzene characters are found to be almost identical up to the fifth hexagon (2). Further, the $\bar{r}_L^P$ values of the kink (1) hexagons of S_5 and 2-S_5 are very similar. Similar features are also found in the $\bar{r}_L^H$ plot. Thus it can be concluded that the local structure of a given hexagon up to the second next hexagons roughly determines its benzene character. Further, if the local structure up to the third next hexagons are the same for two hexagons, either in the same or different molecules, their benzene characters almost coincide within a difference of 0.01. This is also the case with the other benzene characters $\bar{r}_L^H$ and $\bar{b}_L$ and also with more complicated perifusenes.

In Fig. 9 are plotted the $\bar{r}_L^P$ values of the two different sets of compounds, respectively, marked with open and filled circles. In each of the sets the unsymmetrical molecule U is a hybrid of the symmetrical molecules X and O. It is noteworthy that the $\bar{r}_L^P$ values for the larger molecule U_9 (open circles) can accurately be reproduced by the combination of the left half of X_9 and the right half of O_9. For the smaller molecule U_5 (filled circles) agreement is a little less satisfactory for the $\bar{r}_L^P$ values of the central hexagons. Here again the local structure up to the second or third next hexagons seems to determine the benzene character. Quite the same conclusion could be obtained from the values of $\bar{r}_L^H$ and $\bar{b}_L$ just as above.

CONCLUSION

It was found in this study that the three different classes (primary, secondary and tertiary) of hexagons in the catacondensed aromatic hydrocarbons can clearly be distinguished from each other by the combination of the HMO and PPP benzene characters, while for pericondensed aromatic hydrocarbons distinction is less clear but fairly appreciable. One can conclude that the aromatic sextet character of a given benzene ring in a polycyclic aromatic hydrocarbon is determined by the local topological structure around it. Such π-electronic distribution over a given polycyclic system can roughly but easily be estimated from the VB benzene character and the Clar pattern. The concept of the Clar's aromatic

sextet has been interpreted and justified both by the MO and VB theories.

The three benzene characters, $\bar{r}_L^P$, $\bar{r}_L^H$ and $\bar{b}_L$, are thus shown to have their own characteristics in describing the aromatic character of the component hexagons of the polycyclic system and their complementary usage is recommended for analyzing the "higher order π-electronic correlation". It has been established that the π-electronic structure of a long polyene network may well be described by the cooperative interaction of an ensemble of a number of closely correlated pairs of electrons (double bonds) giving rise to the bond alternation. The π-electronic system of a polycyclic aromatic hydrocarbon network may then be described by the cooperative interaction of the units of closely correlated six π-electrons (sextets). Thus the alternancy of the benzene character has been frequently observed in a number of systems studied. This may be the secret of the success of the Clar's postulate. Further analysis of the benzene character in terms of the component molecular orbitals is being under way.

Acknowledgement—Preliminary results of this study have been obtained by Miss Kikuko Hosoi of Ochanomizu University, to whom the authors are greatly indebted.

REFERENCES

[1]A. L. Green, *J. Chem. Soc.* 1886 (1956).
[2]V. E. Sahini, *J. Chim. Phys.* **59**, 177 (1962); A. T. Balaban, *Rev. Roum. Chim.* **15**, 1243 (1970).
[3]N. C. Baird, *Can. J. Chem.* **47**, 3535 (1969).
[4]J. Koutecký, P. Hochman and M. Titz, *J. Chem. Phys.* **70**, 2768 (1966).
[5]H. Gutfreund and W. A. Little, *Phys. Rev.* **183**, 68 (1969); *J. Chem. Phys.* **50**, 4468 (1969).
[6]W. England and K. Ruedenberg, *Theor. Chim. Acta* **22**, 196 (1971).
[7]M. J. S. Dewar and N. Trinajstić, *J. Chem. Soc.* (A) 1220 (1971).
[8]D. M. Hurst and M. E. Linington, *Ibid.* Faraday Trans. 2 **68**, 1988 (1972).
[9]P. Karrer, *Lehrbuch der Organischen Chemie* p. 453. Georg Thieme Verlag, Stuttgart (1950); The term "angularity" is also used. See G. W. Wheland, *Resonance in Organic Chemistry* p. 104. Wiley, New York (1955).
[10]E. Clar, *The Aromatic Sextet*. Wiley, London (1972).
[11]O. E. Polansky and G. Derflinger, *Int. J. Quantum Chem.* **1**, 379 (1967).
[12]H. Sofar, G. Derflinger and O. E. Polansky, *Monatsh. Chem.* **99**, 1895 (1968). See also Refs. 13 and 14.
[13]A. Graovac, I. Gutman, M. Randić and N. Trinajistić, *J. Am. Chem. Soc.* **95**, 6267 (1973).
[14]M. Randić, *Tetrahedron* **30**, 2067 (1974).
[15]W. C. Herndon and M. L. Ellzey, Jr., *J. Am. Chem. Soc.* **96**, 6631 (1974).
[16]M. Randić, *Tetrahedron* **31**, 1477 (1975).
[17]J. Aihara, *Bull. Chem. Soc. Japan.* **49**, 1429 (1976).
[18]H. Hosoya and T. Yamaguchi, *Tetrahedron Letters* 4659 (1975).
[19]K. Nishimoto and L. S. Forster, *Theor. Chim. Acta* **3**, 407 (1965). It was found from a trial calculation that although the component bond order obtained by the geometry-fixed PPP calculation differs from the corresponding value by the variable-β method, the overall MO benzene characters are very similar for the two variant methods. For example, for naphthalene the $\bar{r}_L^P$ values are almost identical with each other. Thus the difference between the $\bar{r}_L^H$ and $\bar{r}_L^P$ values, if any, found in this study may be attributed largely to the electronic repulsion terms.
[20]H. Hosoya and K. Hosoi, *J. Chem. Phys.* **64**, 1065 (1976).
[21]Master thesis of M. A. for Ochanomizu University. Copies of the extensive plots are available on request.
[22]A. T. Balaban and F. Harary, *Tetrahedron* **24**, 2505 (1968).
[23]A. Pullman and B. Pullman, *Cancerisation par les Substances chimiques et Strukture moleculaire*. Masson, Paris (1955).
[24]T. Kanazawa, S. Iwata and H. Hosoya, *Int. J. Quantum Chem.* **15**, 243 (1979).
[25]M. Bradburn, C. A. Coulson and G. S. Rushbrooke, *Proc. Roy. Soc. Edin.* **A62**, 336 (1948).